Effect of Trehalose on W7FW14F Apomyoglobin and Insulin Fibrillization: New Insight into Inhibition Activity†

Silvia Vilasi,‡,§ Clara Iannuzzi,‡,§ Marianna Portaccio,|| Gaetano Irace,‡ and Ivana Sirangelo*,‡

Dipartimenti di Biochimica e Biofisica and Medicina Sperimentale, Seconda Università degli Studi di Napoli, Via L. De Crecchio 7, 80138 Napoli, and Istituto Nazionale Biostrutture e Biosistemi, Viale delle Medaglie d'Oro 305, 00136 Roma, Italy

Received August 1, 2007; Revised Manuscript Received September 25, 2007

ABSTRACT: Trehalose, a disaccharide present in many nonmammalian species, protects cells against various environmental stresses. Trehalose has recently been shown to decrease aggregate formation and toxicity in cell models and to alleviate amyloid-induced diseases. The aim of our study was to use two amyloid-forming proteins, i.e., W7FW14F apomyoglobin and insulin, as model systems to elucidate the molecular mechanism by which trehalose affects the amyloid aggregation process and to investigate further its therapeutic potential. Protein aggregation was examined by far-UV circular dichroism, UV absorption, thioflavin T fluorescence, sodium dodecyl sulfate−polyacrylamide gel electrophoresis, atomic force microscopy, and Fourier transform infrared spectroscopy. Cell viability was investigated by 3-(4,5-dimethylthiazol-2-yl)-2,5-diphenyltetrazolium bromide reduction assay. We found that trehalose does not inhibit protein aggregation but acts at different stages of the fibrillization process depending on the protein model used. In fact, trehalose dose-dependently inhibited fibril formation in the W7FW14F apomyoglobin model and increased the lag phase in the insulin model. In both cases, trehalose caused accumulation of toxic oligomeric species. The results suggest that trehalose may favor or inhibit the formation of "on-pathway" or "off-pathway" oligomeric intermediates depending on the nature of the aggregating protein.

Trehalose (α-D-glucopyranosyl α-D-glucopyranoside) is a naturally occurring disaccharide with protein- and membrane-stabilizing capability (*1*−*6*). Attention has recently focused on its use in the treatment of neurodegenerative diseases associated with protein misfolding and aggregation (*7*−*9*). These diseases, including Alzheimer's, Huntington's, Parkinson's, and prion diseases, are generally associated with the formation of amyloid deposits of proteins/peptides arranged in fibers with a characteristic cross-*β* structure (*10*, *11*). The conversion of globular proteins into insoluble fibrillar aggregates requires significant conformational changes that in most cases are facilitated by amino acid mutations that destabilize the native state and increase the structural flexibility of the peptide chain. However, other proteins are amyloidogenic in the wild-type form (*12*, *13*).

The formation of amyloid fibrils has many of the characteristics of a "nucleated growth" mechanism. The conversion of a protein into its fibrillar form typically includes a lag phase that is followed by a phase of rapid exponential growth (*14*−*16*). The lag phase is assumed to be the time required for "nuclei" to form. Once a nucleus is formed, fibril growth is thought to proceed rapidly by a further association of either monomers or oligomers with the nucleus. While insoluble aggregates correlate with disease progression, there is increasing evidence that the initiating and most toxic events are caused by prefibrillar forms rather than by mature fibrils (*17*−*21*).

Trehalose is a promising drug for the treatment of polyglutamine diseases. In fact, it inhibited polyglutamine-mediated protein aggregation in vitro, reduced aggregate formation and toxicity in cell models, and alleviated polyQ-induced pathology in the R6/2 mouse model of Huntington's disease (*7*, *22*). This protective effect was attributed to trehalose binding to expanded polyQ, which resulted in stabilization of the partially unfolded mutant protein. Similar results were obtained in oculopharyngeal muscular dystrophy, an autosomal dominant disease caused by the abnormal expansion of a polyalanine tract within the coding region of poly(A) binding protein nuclear 1 (PABN1) (*9*). Also in this case, aggregate formation and toxicity were inhibited by trehalose. Finally, trehalose also seems to inhibit insulin amyloid formation (*23*).

Notwithstanding the beneficial effects reported for trehalose, in vitro studies of A*β*40 and A*β*42 showed that its effects on protein aggregation depend on the type of protein being studied. In fact, when coincubated with A*β*40, trehalose inhibits the formation of both fibrillar and prefibrillar oligomeric species, whereas when coincubated with A*β*42, it inhibits the formation of fibrillar aggregates alone. In the latter case, trehalose generates a buildup of small, highly

† This work has been supported by a grant from the Ministero dell'Università e della Ricerca Scientifica e Tecnologica (PRIN 2006), FIRB Grant No. RBNE03PX83 (INBB Unit), and a grant from Regione Campania (DGR 2270, Dec 30, 2006).

* To whom correspondence should be addressed. Phone: +39-81-5667637. Fax: +39-81-5665863. E-mail: ivana.sirangelo@unina2.it.

‡ Dipartimento di Biochimica e Biofisica, Seconda Università degli Studi di Napoli.

§ Joint first authors.

|| Dipartimento di Medicina Sperimentale, Seconda Università degli Studi di Napoli.

10.1021/bi701530w CCC: $40.75
Published on Web 01/19/2008

cytotoxic globular structures (*8*). In this respect, the real effect of trehalose on protein aggregation is still far from being completely understood.

We have used two amyloid-forming proteins, i.e., W7FW14F apomyoglobin and insulin, as models in the attempt to elucidate the molecular mechanism by which trehalose affects amyloid aggregation and to investigate further its therapeutic potential. W7FW14F apomyoglobin aggregates and forms amyloid fibrils under physiological conditions, i.e., neutral pH and room temperature (*24*). Conversely, insulin aggregates at acidic pH and temperatures above 50 °C (*25*, *26*). However, in both cases, aggregation involves monomeric molecules that retain predominantly helical structures, and the formation of highly ordered fibrils results from a structural reorganization of the monomers within the early aggregates (*27*, *28*). Our results demonstrate that trehalose does not inhibit protein aggregation but affects different steps of amyloid fibril formation depending on the protein model used. In fact, trehalose dose-dependently inhibited fibril formation in the W7FW14F apomyoglobin model and increased the lag phase in the insulin model. In both cases, trehalose caused accumulation of toxic oligomeric species. Consequently, caution should be exercised in using trehalose as an amyloid-blocking agent in the clinical setting.

EXPERIMENTAL PROCEDURES

Protein Samples. The W7FW14F myoglobin mutant was expressed in *Escherichia coli* M15 [pREP4] strain as amino-terminal His-tagged forms and purified as previously described (*24*). The protein was sequestered into insoluble inclusion bodies and purified via affinity chromatography on Ni^{2+}−nitrilotriacetic acid resin (Qiagen) under denaturing conditions. Refolding was achieved by removing denaturant by dialysis against 10 mM NaH_2PO_4, pH 2.0, containing decreasing concentrations of urea. The purity of the protein sample was assessed by SDS−PAGE.[1] Protein concentration was determined by measuring the absorbance at 275 nm using extinction coefficients of $\epsilon_{275} = 3750\ M^{-1}{\cdot}cm^{-1}$. The assembly into fibrils was achieved by raising the pH of a 40 μM protein solution to 7.0; this results in the formation of protein aggregates in a prefibrillar form that turn into mature fibrils in 7−15 days (*20*). Trehalose (kindly donated by Dermofarma Italia) was added to the protein solution before the pH was raised to neutrality.

Insulin from bovine pancreas was purchased from Sigma Chemical Co. (St. Louise, MO) and used without further purification. Amyloid aggregation was achieved with a 2 mg/mL stock solution in glycine buffer (pH 2.0, 20 mM), diluted 1:1 with a solution containing different trehalose concentrations or with glycine buffer as a control. The protein samples were incubated at 50, 60, and 75 °C, and aliquots were removed at different times after initiation of the heat treatment.

Spectroscopic Measurements. Circular dichroism (CD) spectra were recorded at 25 °C on a Jasco J-715 spectropolarimeter using thermostated quartz cells of 0.1 cm. Spectral acquisition was carried out at 0.2 nm intervals with a 4 s integration time and a bandwidth of 1.0 nm. An average of three scans was obtained for all spectra. Photomultiplier absorbance did not exceed 600 V in the spectral region analyzed. Data were corrected for buffer contributions and smoothed using the software provided by the manufacturer (system software, version 1.00). All measurements were performed under nitrogen flow. The protein concentration was 20×10^{-6} M. The results were expressed as the mean residue ellipticity, $[\Theta]_{MRW}$ (deg cm^2 $dmol^{-1}$). Absorbance measurements were performed at 25 °C on a Jasco V-550 double beam spectrophotometer.

Thioflavin T (ThT) Fluorescence Measurements. Thioflavin T fluorescence was determined with a Perkin-Elmer Life Sciences LS 55 spectrofluorimeter at excitation and emission wavelengths of 450 and 482 nm, respectively. The excitation and emission slit widths were set at 5 nm each. ThT stock solution was prepared in Tris buffer (pH 8.0, 20 mM) at a concentration of 500 μM and stored at 4 °C. Samples (20 μM) were mixed with a ThT working solution at 50 μM in a quartz cuvette. The fluorescence intensity at 482 nm was corrected by subtracting the emission intensity recorded before the addition of protein to thioflavin T solutions.

FTIR Measurements. Fourier transform infrared spectra were recorded on a Multiscope FT-IR microscope coupled with a Spectrum One spectrometer (Perkin-Elmer, Wellesley, MA). The FTIR spectra in transmission mode were collected (4000−600 cm^{-1} range) at a resolution of 4 cm^{-1} with 16 accumulations per run. For each spectrum, signals corresponding to the water and CO_2 vapors were automatically subtracted and the baseline was corrected. Spectra were recorded with dry samples of W7FW14F apomyoglobin obtained through repeated cycles of lyophilization and dissolution in D_2O at a concentration of 40 μM. Decomposition of the spectra was carried out by using SpectraMax software (Joben-Yvon Inc., Edison, NJ). The software corrects the spectra for the baseline using different polynomial models and performs a best fit procedure to determine spectral deconvolution with Gaussian curves with optimized intensity, position, and width. The goodness of fit is evaluated by means of the χ^2 parameter, and the Levenberg−Marquardt algorithm iteratively adjusts every variable for each peak in an attempt to minimize the χ^2 parameter.

Atomic Force Microscopy. Atomic force microscopy (AFM) images of W7FW14F apomyoglobin samples in the presence of trehalose were recorded on an SPM microscope from Topometrix Corp. (Santa Clara, CA) equipped with a 7 μm scanner and rectangular silicon cantilevers 100 μm long with resonant frequencies in the range 200−300 kHz. AFM images were recorded at a scan rate of 1−10 lines/s. The cantilevers had integrated tips with a curvature radius of 10 nm and a tip cone angle of 35°. The samples were diluted to a concentration of 50 nM in 2 mM $MgCl_2$, and then 10−20 μL of protein solution was immediately deposited onto freshly cleaved ruby mica. The samples were incubated for 2 min, rinsed with water, and blown dry with nitrogen at 0.5 bar.

Cell Culture and Incubation with Protein Aggregates. NIH-3T3 cells (mouse fibroblasts, American Type Culture Collection) were cultured in Dulbecco's modified Eagle's medium (DMEM)-high glucose supplemented with 10% bovine calf serum and 3.0 mM glutamine in a 5.0% CO_2

[1] Abbreviations: UV CD, ultraviolet circular dichroism; ThT, thioflavin T; SDS−PAGE, sodium dodecyl sulfate−polyacrylamide gel electrophoresis; AFM, atomic force microscopy; MTT, 3-(4,5-dimethylthiazol-2-yl)-2,5-diphenyltetrazolium bromide; FTIR, Fourier transformed infrared.

humidified environment at 37 °C. Penicillin (50 units/mL) and streptomycin (50 μg/mL) were added to the medium. The cells were plated at a density of 100 000 cells/well on 12-well plates in 1 mL of medium. After 24 h, the protein samples were diluted at a final concentration of 20 μM in culture medium and added to cell media containing the trehalose concentration being analyzed. Cells incubated with culture medium without protein in the absence and in the presence of trehalose served as the control.

MTT Assay. Cell viability was assessed as the inhibition of the ability of cells to reduce the metabolic dye 3-(4,5-dimethylthiazol-2-yl)-2,5-diphenyltetrazolium bromide (MTT) to a blue formazan product (*29*). After 24 h of incubation with protein samples, the cells were rinsed with phosphate buffer solution (PBS). A 100 μL portion of a stock MTT solution (5 mg/mL in PBS) was then added to 900 μL of DMEM without phenol red containing 10% bovine calf serum/well, and incubation was continued at 37 °C for an additional 3 h. The medium was aspirated, and the cells were treated with isopropyl alcohol−0.1 M HCl for 20 min. Levels of reduced MTT were determined by measuring the difference in absorbance at 570 and 690 nm. Data are expressed as the average percent reduction of MTT with respect to the control ± SD from five independent experiments carried out in triplicate. For statistical analysis, a two-tailed Student's *t* test with unequal variance at a significance level of 5%, unless otherwise indicated, was used.

RESULTS

Trehalose is considered a chemical chaperone because of its ability to modulate protein folding and to inhibit aggregate formation (*1*, *30*). In particular, trehalose has been reported to reduce the extent of polyglutamine, insulin, and Aβ 1−42 amyloid aggregation in vitro (*8*, *22*, *23*). Because this conclusion was based on the absence of fibrils, we investigated the effect of trehalose on the molecular mechanisms leading to aggregation and fibril formation of two amyloid-forming proteins, i.e., W7FW14F apomyoglobin and insulin.

W7FW14F Apomyoglobin Aggregation. We investigated the activity of trehalose as an inhibitor of amyloid aggregation using CD, absorbance measurements, ThT fluorescence, FTIR, and AFM. We first studied the effect of trehalose on the early events of W7FW14F apomyoglobin aggregation using far-UV CD. In mildly acidic conditions, namely, pH 4.0, the amyloid-forming W7FW14F apomyoglobin mutant adopts a soluble partially folded conformation similar to that of the wild-type protein, whereas an increase to pH 7.0 causes protein aggregation and amyloid formation instead of resulting in the formation of the soluble native state (*24*). We recorded CD spectra immediately after pH neutralization of the partially folded conformation with and without increasing concentrations of trehalose, and spectra were then recorded over time. Figure 1 shows the time dependence of the molar ellipticity at 208 nm in the first 6 h of the aggregation process. In the absence of trehalose, the CD intensity gradually decreased over time, and the data were well fitted to a logarithmic function (*28*). The reduction in 208 nm ellipticity was progressively less evident in samples incubated with increasing trehalose concentrations. At 600 mM, trehalose prevented the decrease of negative ellipticity observed in the absence of sugar. The decrease of the CD signal is

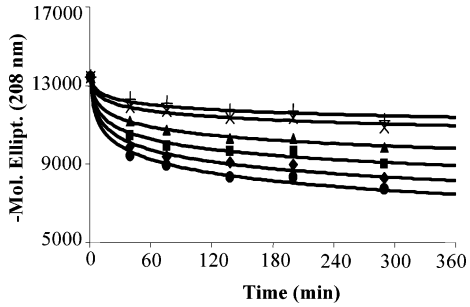

FIGURE 1: Time dependence of the far-UV CD activity at 208 nm of the amyloid-forming W7FW14F apomyoglobin mutant at pH 7.0 in the absence and in the presence of different concentrations of trehalose. The protein concentration was 20×10^{-6} M. Trehalose concentrations were 0 M (●), 50 mM (◆), 100 mM (■), 200 mM (▲), 400 mM (×), and 600 mM (+). Data were interpolated to a logarithmic function as $[\theta](t) = [\theta]_0 + A \ln t$. Points are experimental values; the continuous line was obtained from the logarithmic fit.

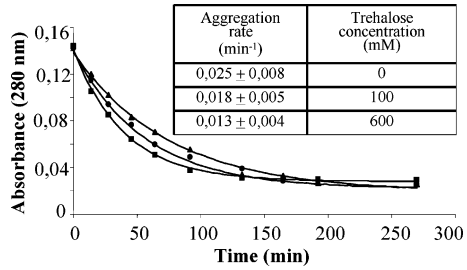

FIGURE 2: Time dependence of W7FW14F apomyoglobin aggregation at pH 7.0 in the absence (■) and in the presence of 100 mM (●) and 600 mM (▲) trehalose. Aggregation was monitored by measuring the absorbance at 280 nm of the supernatant solution after centrifugation. The protein samples were centrifuged at 20000*g* for 30 min. The protein concentration was 40×10^{-6} M. Points are experimental values; continuous lines were obtained from an exponential fit as $y(t) = a + be^{-kt}$. The inset shows the aggregation rates (k) calculated from the fits.

the sum of at least two distinct phenomena: on one hand, the CD signal is sensitive to the change in secondary structure that accompanies amyloid fibril formation; on the other, it reflects the effect of the scatter due to protein aggregation (*28*). In the case of the amyloid aggregation of W7FW14F apomyoglobin, the two factors reacted in a similar fashion. In fact, the intensity of light scatter, which determines loss of the CD signal, is expected to increase with protein aggregation. The apomyoglobin negative ellipticity also decreases when the protein becomes less helical because of the formation of the cross-β amyloid conformation (*28*).

To gain further insight into the effect induced by trehalose, we next measured the protein concentration in the soluble fraction during the early stages of the aggregation process. Protein samples were centrifuged at 20000*g* for 30 min to obtain a supernatant containing prevalently soluble protein. As shown in Figure 2, trehalose did not affect the concentration of the soluble protein fraction, which remained stable at 15% total protein 6 h after the onset of aggregation, thus indicating that aggregation was not prevented. Similarly trehalose did not significantly affect the aggregation rate, obtained by fitting the experimental data to an exponential function as $y(t) = a + be^{-kt}$ (Figure 2, inset). Taken together, the results reported in Figures 1 and 2 indicate that trehalose does not suppress the early phase of W7FW14F apomyoglobin amyloid aggregation. In this respect, the limited

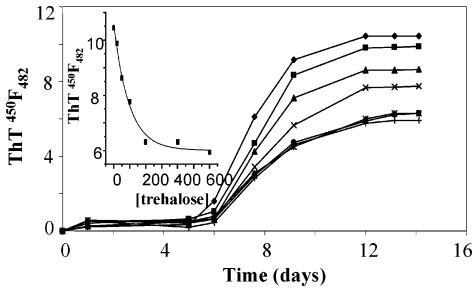

FIGURE 3: W7FW14F apomyoglobin fibrillization monitored by ThT fluorescence emission in the absence and in the presence of different concentrations of trehalose. The protein concentration was 20×10^{-6} M, the ThT concentration was 50×10^{-6} M, and the trehalose concentrations were 0 M (◆), 20 mM (■), 50 mM (▲), 100 mM (×), 200 mM (*), 400 mM (●), and 600 mM (+). The inset shows the dependence of the ThT fluorescence intensity at 14 days on the trehalose concentration.

decrease of negative CD ellipticity can be ascribed to a conformational effect.

To evaluate the effect of trehalose on amyloid aggregation of W7FW14F apomyoglobin over a longer time, we carried out a series of experiments using ThT fluorescence spectroscopy. This dye binds the β-cross structure, thereby causing a strong increase of its fluorescence emission at 480 nm (*31*). In the absence of trehalose, W7FW14F apomyoglobin shows a time-dependent increase of ThT fluorescence with a characteristic lag time as the protein begins to aggregate and form oligomeric structures (Figure 3). Incubation of W7FW14F apomyoglobin with trehalose did not affect ThT fluorescence during the lag phase. The samples incubated with trehalose had the same ThT fluorescence intensity as the control, thereby confirming that trehalose does not suppress the early phase of the aggregation process. After a lag period of 6 days, the fluorescence intensity increased but did not reach the maximal value recorded at the stationary phase, which indicates that trehalose inhibits the formation of fibrils from early aggregates in a dose-dependent manner. At a concentration of 200 mM, trehalose inhibited fibril formation by about 50% (Figure 3, inset). Higher concentrations of trehalose did not increase the magnitude of fibril inhibition.

To obtain additional information about the fibrillization inhibitory properties of trehalose, we incubated the amyloidogenic apomyoglobin with the sugar for 15 days. The protein samples were then centrifuged at 20000*g* for 10 min to separate fibrillar structures from nonfibrillar aggregates, and the pellet and supernatant fractions were analyzed by SDS−PAGE. As the concentration of trehalose increased, the band relative to the pellet fraction was less intense than that observed in the absence of sugar (Figure 4). This result is fully consistent with the data reported in Figure 3 showing that higher trehalose concentrations decrease the magnitude of fibril formation.

We next examined the morphologies of the W7FW14F apomyoglobin aggregates obtained in the presence of 600 mM trehalose by AFM (Figure 5). As expected, 15 days after the onset of the aggregation process, mature fibrils appeared in the control sample (no trehalose). In contrast, granular species predominated in the protein sample incubated with trehalose. Consistent with the ThT staining results, the AFM images show that the formation of fibrils is inhibited in the

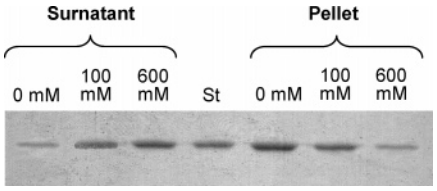

FIGURE 4: Effect of trehalose on W7FW14F apomyoglobin aggregation analyzed by SDS−PAGE. Aliquots of protein, in the absence and in the presence of 100 and 600 mM trehalose, were taken 15 days from the beginning of the aggregation process and centrifuged at 20000*g* for 10 min. The pellet and surnatant were loaded onto 12% acrylamide gel and stained with Coomassie Blue.

presence of trehalose, whereas the formation of prefibrillar oligomeric structures is not affected.

Direct information on the structure of W7FW14F apomyoglobin aggregates formed in the presence of trehalose was obtained with FTIR spectroscopy, which is a very sensitive technique that is widely used to monitor the α to β transition underlying amyloid formation (*32*, *33*). Figure 6 shows the spectra recorded 15 days after the onset of the aggregation reaction performed in the absence and in the presence of trehalose. The deconvolution analysis of the amide I region in the absence of trehalose revealed a Gaussian component (40% of the total) centered at 1621 cm^{-1}, which is typical of the cross-β amyloid conformation (*34*). Trehalose reduces this component by as much as 10% and results in a Gaussian component centered at 1636 cm^{-1} (30%). This value typically belongs to the range commonly assigned to the β sheet native conformation (*34*). This result suggests that the conversion of the β sheet native structure, probably present in early oligomers, into a cross-β amyloid structure is inhibited in the presence of trehalose. This is in line with the lack of a decrease in the CD signal at 208 nm observed in the presence of trehalose (see Figure 1).

W7FW14F Apomyoglobin Cytotoxicity. We investigated the effect of trehalose on the cytotoxicity of W7FW14F apomyoglobin aggregates using the MTT assay. This is a rapid, sensitive indicator of amyloid-mediated toxicity. The toxicity of amyloid aggregates is closely linked to oligomeric morphologies. Indeed, soluble prefibrillar oligomers, but not mature fibrils, generally cause a decrease in reduced MTT concentrations (*12*, *17*−*21*). We evaluated the toxicity associated with aggregates formed in the absence and in the presence of different trehalose concentrations at the onset of aggregation and 15 days thereafter. As shown in Figure 7, the MTT reduction level decreased significantly to 60% ($p < 0.001$) of the control level when cells were exposed for 24 h to early W7FW14F apomyoglobin prefibrillar aggregates formed in both the presence and absence of trehalose. Samples exposed to the higher trehalose concentrations tested, i.e., 100 and 200 mM, were cytotoxic even after 15 days of incubation, which indicates the persistence of the oligomeric prefibrillar structures. At a lower trehalose concentration, i.e., 20 mM, the level of MTT reduction was similar to that of the control. The decrease of MTT activity well correlates with the ThT fluorescence data (Figure 3) and suggests that the lack of cytotoxicity may be a marker of harmless mature fibrils. Taken together, our results indicate that trehalose inhibits fibril formation and maintains the aggregates in a nonfibrillar, highly cytotoxic state.

Insulin Aggregation and Cytotoxicity. Insulin amyloid formation, like other amyloidogenic proteins, occurs through

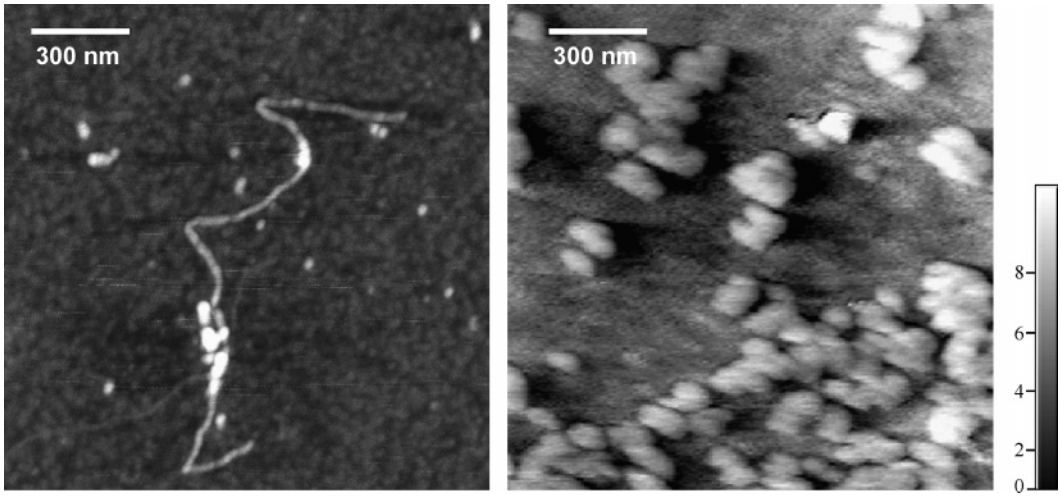

FIGURE 5: W7FW14F apomyoglobin fibrillization in the absence (left) and in the presence (right) of trehalose monitored by AFM. The scale represents height of pixels in the image. The protein samples were taken 15 days from the beginning of the aggregation process.

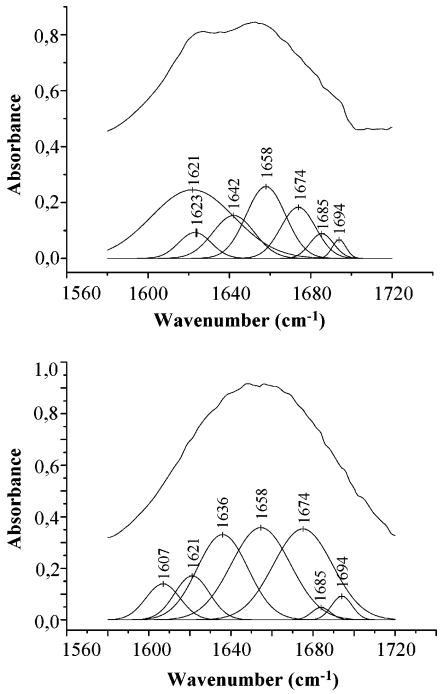

FIGURE 6: FTIR spectra of amyloid-forming W7FW14F apomyoglobin in the amide I′ region at pH 7.0 in the absence (upper) and in the presence (lower) of 600 mM trehalose after 15 days from the beginning of the aggregation process. Spectra were corrected for the baseline and decomposed with Gaussian curves.

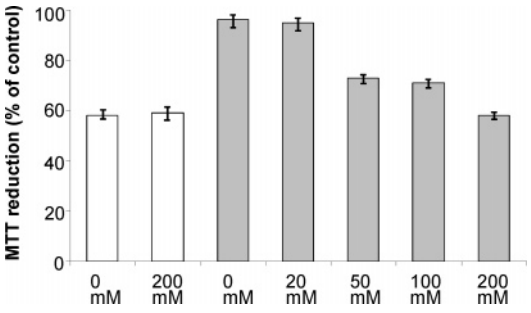

FIGURE 7: Toxicity of W7FW14F apomyoglobin aggregates formed in the absence and in the presence of different trehalose concentrations. The cells were exposed for 24 h to W7FW14F apomyoglobin aggregates formed at the beginning of the aggregation process (white columns) and after 15 days (gray columns). The viability of the cells was measured using MTT assay. Data are expressed as the average percentage of MTT reduction ± SD relative to that of cells treated with medium alone or medium plus trehalose from triplicate wells from five separate experiments. The protein concentration was 20 μM.

a nucleation and elongation process, and its rate is remarkably increased under stress conditions such as high temperature and extreme pH (*35*−*37*). Small stress molecules, including trehalose, have been shown to inhibit amyloid formation of insulin in vitro (*23*). Specifically, the effect of trehalose was monitored by ThT fluorescence for 40 h at a preincubation temperature of 50 °C. Under these experimental conditions, there was no increase in ThT fluorescence, and AFM images showed a population of small granular aggregates and rare fibrils (*23*). However, cytotoxicity studies on the trehalose effect were not performed.

To elucidate better the inhibitory property of trehalose, we tested its effect on insulin amyloid aggregation by measuring ThT fluorescence at different preincubation temperatures, i.e., 50, 60, and 75 °C (Figure 8). Application of heat stress shortened the lag time for amyloid fibril formation and increased the maximal value of ThT fluorescence during the stationary phase (*23*). In agreement with previous data, fluorescence was not increased after 40 h of incubation at 50 °C with 300 or 600 mM trehalose. However, the typical sigmoidal increase occurred at a longer time (namely, 50 and 75 h, respectively) and reached the same maximal fluorescence value obtained in the absence of trehalose. These data indicate that trehalose lengthens the lag phase but does not suppress amyloid fibril formation from prefibrillar aggregates. A similar effect was observed at preincubation temperatures of 60 and 75 °C. At these temperatures, the increase of the lag phase was less pronounced than at 50 °C. However, at all temperatures tested, higher trehalose concentrations did not affect the maximal ThT fluorescence value. This indicates that trehalose influences the nucleation phase but does not inhibit amyloid fibril formation. Differently, using a shorter observation time, Arora et al. (*23*) found that trehalose completely suppressed insulin amyloid formation. Our data indicate that trehalose keeps the protein in the more toxic prefibrillar conformation for a longer time. We evaluated the viability of cells exposed to insulin aggregates formed at 50 °C for different times with and

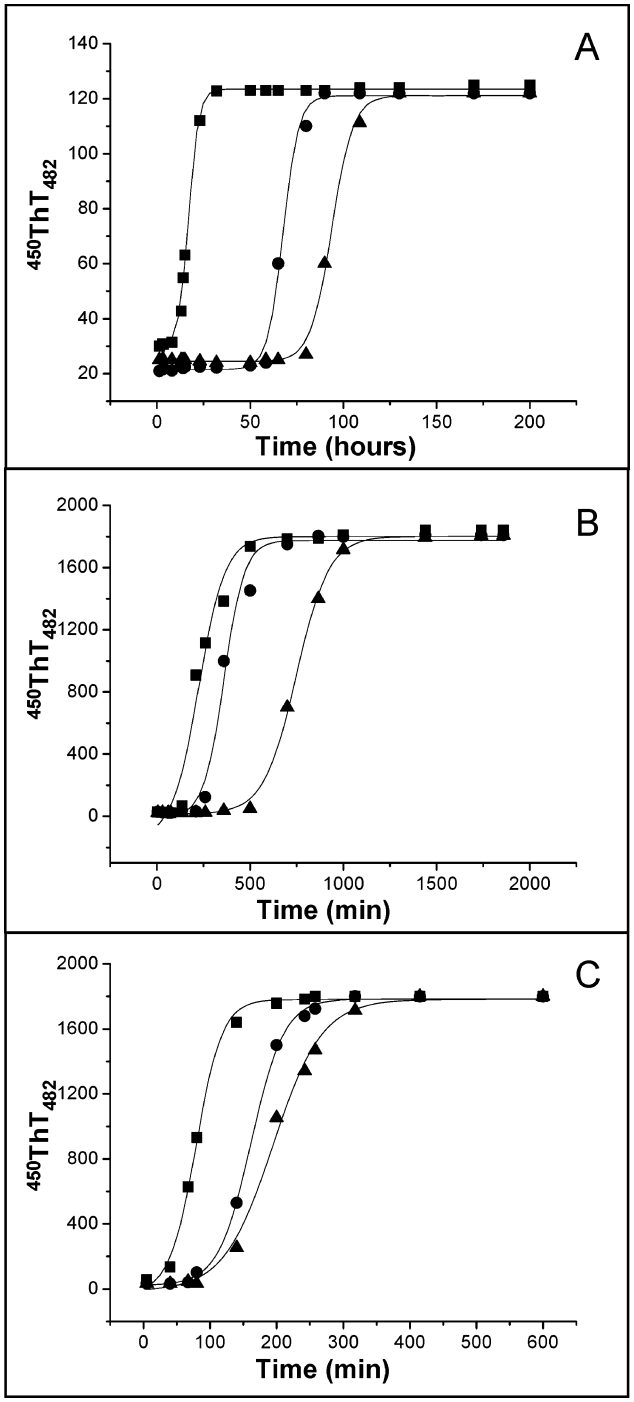

FIGURE 8: Kinetics of insulin fibrillization in the absence and in the presence of different concentrations of trehalose monitored by ThT fluorescence. The protein concentration was 20×10^{-6} M, the ThT concentration was 50×10^{-6} M, and the trehalose concentrations were 0 M (■), 300 mM (●), and 600 mM (▲). The preincubation temperatures were 50 °C (A), 60 °C (B), and 75 °C-(C). Data were interpolated to sigmoidal functions as $y = [A_1 - A_2]/[1 + e^{(x-x_o)/dx}] + A_2$.

without 300 mM trehalose. After 1 h of preincubation at 50 °C, insulin aggregates were highly cytotoxic irrespectively of trehalose (Figure 9), which indicates that toxicity is strictly related to the length of the lag phase. At 24 h, toxicity persisted only in the case of cells exposed to insulin aggregates formed in the presence of trehalose. After 60 h, i.e., at the stationary phase of the fibril formation, all aggregates were harmless.

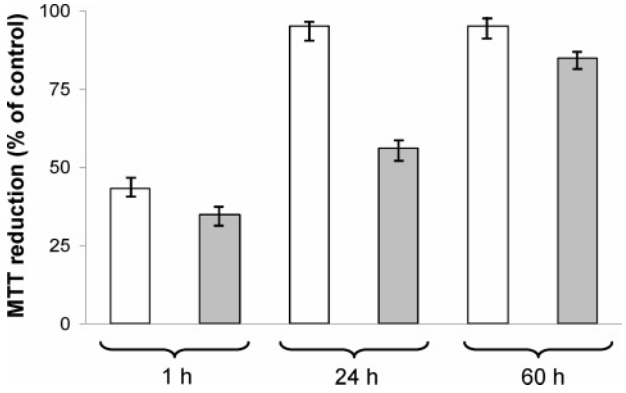

FIGURE 9: Toxicity of insulin aggregates formed at preincubation temperature of 50 °C for 1, 24, and 60 h in the absence (white columns) and in the presence (gray columns) of 300 mM trehalose. The experimental procedures are those reported in Figure 7. The protein concentration was 60 μM.

DISCUSSION

The aim of our study was to gain insight into the effect of trehalose on amyloid aggregation using the amyloidogenic W7FW14F apomyoglobin mutant and insulin as protein models. Before aggregation, the amyloidogenic apomyoglobin mutant adopts a substantially nativelike helical conformation, which rapidly aggregates at neutral pH to form highly cytotoxic prefibrillar oligomeric species (*20*, *24*, *28*). Insulin is a small helical protein consisting of two polypeptide chains, A and B, linked together by two disulfide bridges. When the protein is heated at high temperatures and low pH, a partial unfolding occurs and results in aggregates that initially have a predominantly helical structure (*25*−*27*). At the macroscopic level, these two proteins display a rather similar aggregation pathway consisting of formation of nonfibrillar aggregates, development of prefibrils and protofilaments, and, finally, their assembly into mature fibrils (*24*, *27*).

Here we show that trehalose does not suppress the early stages of the aggregation process during which toxic oligomeric species are formed, but affects the subsequent steps of amyloid fibril formation in different ways depending on the protein model. Our data seem to contrast with reports in which trehalose was described as an in vitro inhibitor of amyloid aggregation (*8*, *22*, *23*). However, there is no real discrepancy because the latter conclusion was based on the absence of fibrillar structures. Moreover, the term "aggregation inhibition" can be misleading because amyloid aggregation is a complex nucleation−polymerization process that begins with toxic oligomeric precursors and continues with their assembly into harmless mature fibrils. Evaluation of potential antiaggregating drugs as therapeutic agents must therefore take into account the entire aggregation process, not only the formation of fibrils.

In the case of amyloidogenic apomyoglobin, trehalose dose-dependently reduced fibril formation without affecting the lag phase. Differently, in the case of insulin, trehalose increased the duration of the lag phase, after which fibril formation took place normally. However, in both instances, trehalose resulted in accumulation of oligomeric toxic species irrespective of the step at which it affected amyloid aggregation. The differences between the two proteins are probably due to the different temperatures at which they were studied,

i.e., 25 °C and above 50 °C for apomyoglobin and insulin, respectively. Our results with insulin differ from those of Arora et al. (*23*), who reported that trehalose suppresses fibril formation. However, they used a shorter observation time and did not carry out a cytotoxicity assay.

Previous studies indicated that trehalose stabilizes proteins from denaturation by a combined effect of increased surface tension of the solution coupled with preferential hydration of protein monomers (*37*−*40*). This forces the protein to retain a compact conformation to minimize the energy of the solvent−protein system. It is difficult to envisage the mechanism by which trehalose influences fibril formation but not protein aggregation. The formation of fibrils requires substantial structural reorganization, and the most highly ordered structures slowly evolve from the initially formed species. In this respect, in line with the water-layer hypothesis (*41*, *42*), it is conceivable that trehalose molecules form a coating layer around oligomeric aggregates that contain essentially nativelike molecules. This reduces the solvation forces, thereby increasing intramolecular interactions. The consequent stabilization of the protein structure inside the oligomer would, therefore, limit any further structural rearrangements that lead to the formation of prefibrils and fibrils with a more extended β-cross structure. This is supported by our finding that the spectral deconvolution of the amyloidogenic apomyoglobin exposed to trehalose for 15 days showed a decrease of the Gaussian component centered at 1621 cm^{-1} which is usually associated with the amyloid cross-β conformation, i.e., 10% vs 40% of the control protein. Our amyloidogenic apomyoglobin results are similar to those of Liu et al. (*8*), who found that trehalose dose-dependently reduces Aβ fibril formation but not the initial aggregation, thereby leading to the formation of oligomeric aggregates. In both cases, trehalose does not seem to prevent aggregation but rather to favor formation of aggregates that do not nucleate fibril formation.

The different effect exerted by trehalose on insulin, namely, delay of fibril formation instead of its inhibition, may be ascribed to the thermal energy increase at higher temperatures, although more information about the protein−trehalose interaction is required to clarify the mechanism underlying this effect. Trehalose may delay fibril formation by stabilizing protein aggregates not able to nucleate fibrils. The increase of kinetic energy occurring at higher temperatures could revert non-nucleating aggregate formation. Increasing evidence indicates that aggregation occurs via multiple pathways that form distinct aggregate species, some of which are "on pathway" intermediates for fibril formation, and others are "off pathway" species. The possibility that the latter species serve to buffer monomer concentration is underdebated (*43*−*46*).

Our data indicate that the effect of trehalose on W7FW14F and insulin consists in a delay or inhibition of fibril formation, thereby maintaining a population of more toxic species. Similar data have been reported for Aβ42 (*8*). In this respect, care should be taken to ensure that strategies aimed at inhibiting fibril formation do not cause a corresponding increase in the concentration of toxic oligomeric species. Nevertheless, it cannot be excluded that trehalose may affect aggregation (and exert its beneficial effects) via mechanisms other than by directly affecting polymerization. In this context, it has recently been reported that trehalose regulates the heat shock transcription factor Hsf1, a key protein in promoting the cellular manufacture of proteins (*47*). Sarkar et al. (*48*) found that trehalose stimulates autophagy, thereby accelerating clearance of such aggregate-prone proteins as mutant huntingtin and α-synuclein, and protects cells from subsequent proapoptotic insults. This process decreases levels of toxic protein fragments and improves survival in laboratory cell models of Huntington's and Parkinson's disease (*48*). In addition, trehalose exerts significant stabilizing effects on membrane structure and function, as has been shown for membranes that are damaged by many other cell stressors (*49*). Moreover, trehalose acts as an antioxidant and free radical scavenger (*50*). It restored calcium homeostasis and improved metabolic parameters in a rat model (*51*). These effects could help to prevent the cellular damage induced by amyloid aggregates.

ACKNOWLEDGMENT

We are grateful to Antonio Carola (Dipartimento di Scienze della Vita, Seconda Università di Napoli) for AFM measurements. Silvia Vilasi thanks Prof. Gliozzi's research group (Dipartimento di Fisica, Università di Genova) for training in the AFM technique. We thank Jean Ann Gilder for text editing.

REFERENCES

1. Singer, M. A., and Lindquist, S. (1998) Multiple effects of trehalose on protein folding in vitro and in vivo, *Mol. Cell 1* (5), 639−648.
2. Xie, G., and Timasheff, S. N. (1997) The thermodynamic mechanism of protein stabilization by trehalose, *Biophys. Chem. 64*, 25−43.
3. Chen, L., Cabrita, G. J. M., Otzen, D. E., and Melo, E. P. (2005) Stabilization of the ribosomal protein S6 by trehalose is counterbalanced by the formation of a putative off-pathway species, *J. Mol. Biol. 351*, 402−416.
4. Colaco, C., Sen, S., Thangavelu, M., Pinder, S., and Roser, B. (1992) Extraordinary stability of enzymes dried in trehalose: simplified molecular biology, *Bio/Technology 10* (9), 1007−1011.
5. Colaco, C., Kampinga, J., and Roser, B. (1995) Amorphous stability and trehalose, *Science 268* (5212), 788.
6. Crowe, J. H., Tablin, F., Wolkers, W. F., Gousset, K., Tsvetkova, N. M., and Ricker, J. (2003) Stabilization of membranes in human platelets freeze-dried with trehalose, *Chem. Phys. Lipids 122* (1−2), 41−52.
7. Tanaka, M., Machida, Y., Niu, S., Ikeda, T., Jana, N. R., Doi, H., Kurosawa, M., Nekooki, M., and Nukina, N. (2004) Trehalose alleviates polyglutamine-mediated pathology in a mouse model of Huntington disease, *Nat. Med. 10* (2), 148−154.
8. Liu, R., Barkhordarian, H., Emadi, S., Park, C. B., and Sierks, M. R. (2005) Trehalose differentially inhibits aggregation and neurotoxicity of beta-amyloid 40 and 42, *Neurobiol. Dis. 20* (1), 74−81.
9. Davies, J. E., Sarkar, S., and Rubinsztein, D. C. (2006) Trehalose reduces aggregate formation and delays pathology in a transgenic mouse model of oculopharyngeal muscular dystrophy, *Hum. Mol. Genet. 15* (1), 23−31.
10. Carrell, R. W., and Lomas, D. A. (1997) Conformational disease, *Lancet 350*, 134−138.
11. Uversky, V. N., and Fink, A. L. (2006) *Protein Misfolding, Aggregation and Conformational Diseases*, Vols. 1 and 2, Kluwer Academic/Plenum, New York.
12. Stefani, M., and Dobson, C. M. (2003) Protein aggregation and aggregate toxicity: new insights into protein folding, misfolding diseases and biological evolution, *J. Mol. Med. 81*, 678−699.
13. Stefani, M. (2004) Protein misfolding and aggregation: new examples in medicine and biology of the dark side of the protein world, *Biochim. Biophys. Acta 1739* (1), 5−25.
14. Serio, T. R., Cashikar, A. G., Kowal, A. S., Sawicki, G. J., Moslehi, J. J., Serpell, L., Arnsdorf, M. F., and Lindquist, S. L. (2000)

Nucleated conformational conversion and the replication of conformational information by a prion determinant, *Science 289*, 1317−1321.
15. Uversky, V. N., Li, J., Souillac, P., Millett, I. S., Doniach, S., Jakes, R., Goedert, M., and Fink, A. L. (2002) Biophysical properties of the synucleins and their propensities to fibrillate: inhibition of alpha-synuclein assembly by beta- and gamma-synucleins, *J. Biol. Chem. 277*, 11970−11978.
16. Pedersen, J. S., Christensen, G., and Otzen, D. E. (2004) Modulation of S6 fibrillation by unfolding rates and gatekeeper residues, *J. Mol. Biol. 341*, 575−588.
17. Bucciantini, M., Giannoni, E., Chiti, F., Baroni, F., Formigli, L., Zurdo, J., Taddei, N., Ramponi, G., Dobson, C. M., and Stefani, M. (2002) Inherent toxicity of aggregates implies a common mechanism for protein misfolding disease, *Nature 416*, 507−511.
18. Bucciantini, M., Calloni, G., Chiti, F., Formigli, L., Nosi, D., Dobson, C. M., and Stefani, M. (2004) Prefibrillar amyloid protein aggregates share common features of cytotoxicity, *J. Biol. Chem. 279*, 31374−31382.
19. Kayed, R., Head, E., Thomson, J. L., Mcintire, T. M., Milton, S. C., Cotman, C. W., and Glabe, C. G. (2003) Common structure of soluble amyloid oligomers implies common mechanism of pathogenesis, *Science 300*, 486−489.
20. Sirangelo, I., Malmo, C., Iannuzzi, C., Mezzogiorno, A., Bianco, M. R., Papa, M., and Irace, G. (2004) Fibrillogenesis and cytotoxic activity of the amyloid-forming apomyoglobin mutant W7FW14F, *J. Biol. Chem. 279*, 13183−13189.
21. Malmo, C., Vilasi, S., Iannuzzi, C., Tacchi, S., Cametti, C., Irace, G., and Sirangelo, I. (2006) Tetracycline inhibits W7FW14F apomyoglobin fibril extension and keeps the amyloid protein in a pre-fibrillar, highly cytotoxic state, *FASEB J. 20* (2), 346−347.
22. Tanaka, M., Makida, Y., and Nukina, N. (2005) A novel therapeutic strategy for polyglutamine diseases by stabilizing aggregation-prone proteins with small molecules, *J. Mol. Med. 83*, 343−352.
23. Arora, A., Ha, C., and Park, C. B. (2004) Inhibition of insulin amyloid formation by small stress molecules, *FEBS Lett. 564*, 121−125.
24. Sirangelo, I., Malmo, C., Casillo, M., Mezzogiorno, A., Papa, M., and Irace, G. (2002) Tryptophanyl substitution in apomyoglobin determine protein aggregation and amyloid-like fibril formation at physiological pH, *J. Biol. Chem. 277*, 45887−45891.
25. Waugh, D. F. (1946) A fibrous modification of insulin: the heat precipitate of insulin, *J. Am. Chem. Soc. 68*, 247−250.
26. Brange, J., Andersen, L., Laursen, E. D., Meym, G., and Rasmussen, E. (1997) Towards understanding insulin fibrillation, *J. Pharm. Sci. 86*, 517−525.
27. Bouchard, M., Zurdo, J., Nettleton, E. J., Dobson, C. M., and Robinson, C. V. (2000) Formation of insulin amyloid fibrils followed by FTIR simultaneously with CD and electron microscopy, *Protein Sci. 9*, 1960−1967.
28. Iannuzzi, C., Vilasi, S., Portaccio, M., Irace, G., and Sirangelo, I. (2007) Heme binding inhibits the fibrillization of amyloidogenic apomyoglobin and determines lack of aggregate cytotoxicity, *Protein Sci. 16* (3), 507−516.
29. Hansen, M. B., Nielsen, S. E., and Berg, K. (1989) Re-examination and further development of a precise and rapid dye method for measuring cell growth/cell kill, *J. Immunol. Methods 119*, 203−210.
30. Welch, W. J., and Brown, R. (1996) Influence of molecular and chemical chaperones on protein folding, *Cell Stress Chaperones 1*, 109−115.
31. Levine, H., III. (1993) Thioflavine T interaction with synthetic Alzheimer's disease beta-amyloid peptides: setection of amyloid aggregation in solution, *Protein Sci. 2*, 404−410.
32. Dzwolak, W., Ravindra, R., Lendermann, J., and Winter, R. (2003) Aggregation of bovine insulin probed by DSC/PPC calorimetry and FTIR spectroscopy, *Biochemistry 42*, 11347−11355.
33. Fandrich, M., Forge, V., Buder, K., Kittler, M., Dobson, C. M., and Diekmann, S. (2003) Myoglobin forms amyloid fibrils by association of unfolded polypeptide segments, *Proc. Natl. Acad. Sci. U.S.A. 100*, 15463−15468.
34. Zandomeneghi, G., Krebs, M. R.H., Mccammon, M. G., and Fandrich, M. (2004) FTIR reveals differences between native β-sheet proteins and amyloid fibrils, *Protein Sci. 13*, 3314−3321.
35. Jimenez, J. L., Nettleton, E. J., Bouchard, M., Robinson, C. V., Dobson, C. M., and Saibil, H. R. (2002) The protofilament structure of insulin amyloid fibrils, *Proc. Natl. Acad. Sci. U.S.A. 99*, 9196−9201.
36. Arora, A., Ha, C., and Park, C. B. (2004) Insulin amyloid fibrillation at above 100 °C: new insights into protein folding under extreme temperatures, *Protein Sci. 13*, 2429−2436.
37. Nielsen, L., Khurana, R., Coats, A., Frokjaer, S., Brange, J., Vyas, S., Uversky, V. N., and Fink, A. L. (2001) Effect of environmental factors on the kinetics of insulin fibril formation: elucidation of the molecular mechanism, *Biochemistry 40*, 6036−6046.
38. Melo, E. P., Faria, T. Q., Martins, L. O., Goncalves, A. M., and Cabral, J. M. S. (2001) Cutinase unfolding and stabilization by trehalose and mannosylglycerate, *Proteins 42*, 542−552.
39. Gekko, K., and Timasheff, S. N. (1981) Mechanism of protein stabilization by glycerol: preferential hydration in glycerol-water mixtures, *Biochemistry 20*, 4667−4676.
40. Arakawa, T., and Timasheff, S. N. (1982) Stabilization of protein structure by sugars, *Biochemistry 21*, 6536−6544.
41. Belton, P. S., and Gil, A. M. (1994) IR and Raman spectroscopic studies of the interaction of trehalose with hen egg white lysozyme, *Biopolymers 34*, 957−961.
42. Lins, R. D., Pereira, C. S., and Hunenberger, P. H. (2004) Trehalose-protein interaction in aqueous solution, *Proteins 55*, 177−186.
43. Lomakin, A., Chung, D. S., Benedek, G. B., Kirschner, D. A., and Teplow, D. B. (1996) On the nucleation and growth of amyloid β-protein fibrils: Detection of nuclei and quantitation of rate constants, *Proc. Natl. Acad. Sci U.S.A. 93*, 1125−1129.
44. Harper, J. D., Wong, S. S., Lieber, C. M., and Lansbury, P. T., Jr. (1999) Assembly of Aβ amyloid protofibrils: An in vitro model for a possible early event in Alzheimer's disease, *Biochemistry 38*, 8972−8980.
45. Necula, M., Kayed, R., Milton, S., and Glabe, C. G. (2007) Small molecule inhibitors distinguish between amyloid β oligomerization and fibrillization pathways, *J. Biol. Chem. 282*, 10311−10324.
46. Necula, M., Breydo, L., Milton, S., Kayed, R., van der Veer, W. E., Tone, P., and Glabe, C. G. (2007) Methylene blue inhibits amyloid Aβ oligomerization by promoting fibrillization, *Biochemistry 46*, 8850−8860.
47. Conlin, L. K., and Nelson, H. C. M. (2007) The natural osmolyte trehalose is a positive regulator of the heat-induced activity of yeast heat shock transcription factor, *Mol. Cell. Biol. 27* (4), 1505−1515.
48. Sarkar, S., Davies, J. E., Huang, Z., Tunnacliffe, A., and Rubinsztein, D. C. (2007) Trehalose, a novel mTOR-independent autophagy enhancer, accelerates the clearance of mutant huntingtin and alpha-synuclein, *J. Biol. Chem. 282*, 5641−5652.
49. Elbein, A. D., Pan, T, Y., Pastuszak, I., and Carroll, D. (2003) New insights on trehalose: a multifunctional molecule, *Glycobiology 13* (4), 7−27.
50. Oku, K., Kurose, M., Kubota, M., Fukuda, S., Kurimoto, M., Tujisaka, Y., Okabe, A., and Sakurai, M. (2005) Combined NMR and quantum chemical studies on the interaction between trehalose and dienes relevant to the antioxidant function of trehalose, *J. Phys. Chem. B 109* (7), 3032−3040.
51. Nguyen, H. P., Bonin, M., Stephan, M., Kuhn, M., Holzmann, C., Reilmann, R., von Horsten, S., and Rieb, O. (2006) Trehalose treatment restores calcium homeostasis in transgenic rat model of Huntington's disease, *Proceedings of Neurodegenerative Diseases: Molecular Mechanisms in a Functional Genomics Framework*, Max Delbrueck Center, Berlin-Buch, September 6−9, 2006; Abstract 48.

BI701530W